

Application of response surface methodology (RSM) for optimization of the supercritical CO₂ extract of oil from *Zanthoxylum bungeanum* pericarp: Yield, composition and gastric protective effect

Mengmeng Zhang¹, Daneng Wei¹, Lin He, Dan Wang, Li Wang, Dandan Tang, Rong Zhao, Xun Ye, Chunjie Wu^{*}, Wei Peng^{*}

State Key Laboratory of Southwestern Chinese Medicine Resources, School of Pharmacy, Chengdu University of Traditional Chinese Medicine, Chengdu 611137, PR China

ARTICLE INFO

Keywords:

Z. bungeanum
SC-CO₂
Composition analysis
Gastric protective effect
Serum metabolomics

ABSTRACT

Supercritical carbon-dioxide (SC-CO₂) is a promising two-phase technology for flavor components (volatile oil and alkylamides) extract from *Zanthoxylum bungeanum* pericarp. However, the gastric protective effect of SC-CO₂ extract from *Z. bungeanum* (SZB) have not been systematically investigated. In this study, response surface methodology (RSM) was employed to optimize the yield of SZB, and the average yield of 11.07 % were obtained under optimal parameters (30 MPa, 43 °C and time 75 min). Here, limonene, linalool and hydroxy- α -sanshool were identified as the main compounds of SZB by GC-MS and UPLC-Q-Extractive Orbitrap/MS analysis. When the gastric protective effect of SZB (5, 10 and 20 mg/kg, p.o.) were evaluated, significant increase in body weight and organ indexes of rat, and decreased gastric lesion were observed. Furthermore, nineteen serum metabolites were regarded as the potential biomarkers for the gastric protective effect of SZB. Collectively, this study provides a comprehensive perspective into the chemical composition analysis and gastric protective effect of *Z. bungeanum* SC-CO₂ extract.

Introduction

Zanthoxylum bungeanum (Rutaceae family), known as *Huā Jiāo* in Chinese, is widely distributed in East Asia including China, Japan, and Korea, and has a long cultivation history over 2000 years in China (Zhang et al., 2017). The ripened pericarp of *Z. bungeanum* is a widely consumed spice and one of “eight essential condiments” in cooking with a characteristic aroma and tingling flavor. Used as a spice, a few granules, powder, and seasoning oil is often added together with peppers in Chinese cuisine, such as Sichuan hotpot and *mapo tofu*, to generate a wonderful flavor of *málà* (Ni, Yan, Tian, Zhan, & Zhang, 2022). It is worth noting that since the Shen Nong’s Herbal Classic, *Z. bungeanum* pericarp has proven to be a valuable source for protecting gastric from eating raw and cold food and its complication of emesis and diarrhea. Kubota et al. (2015) reported that hydroxy- α -sanshool, a main

component of alkylamides, has been found to increase defecation frequency in normal and laparotomy rats, possibly via blockage of the neural KCNK9 channel (Kubota et al., 2015). As a major volatile oil component, limonene showed effective gastroprotection against lesions induced by absolute ethanol, due to an increase in the gastric mucus production induced by conserving the basal PGE₂ levels (Moraes et al., 2009).

These findings suggested that volatile oil and unsaturated alkylamides may be the active fraction from *Z. bungeanum* for the gastric protective effect. It is limited to obtain high yield of these two types of components together by the conventional methods of water decoction and organic solvents extraction. While supercritical carbon-dioxide (SC-CO₂) with CO₂ as the supercritical fluid has been receiving growing interest in food and pharmaceutical industries in modern times (Zhao, Xu, Wang, & Zhao, 2021). As a green approach, it is utilized to extract

Abbreviations: BBD, Box-Behnken Design; CGRP, Calcitonin gene related peptide; HESI, Heated electrospray ionization; MS, Mass spectra; PCA, Principal component analysis; PLS-DA, Partial least squares-discriminate analysis; QC, Quality control; RI, Retention index; RSM, Response surface methodology; SC-CO₂, Supercritical carbon-dioxide; SZB, SC-CO₂ extract from *Zanthoxylum bungeanum*; SP, Substance P; VIP, Variable importance in the projection.

^{*} Corresponding authors.

E-mail addresses: wucjcdctm@163.com (C. Wu), pengwei@cdutcm.edu.cn (W. Peng).

¹ These authors are equal contribution to this work.

<https://doi.org/10.1016/j.fochx.2022.100391>

Received 12 April 2022; Received in revised form 6 July 2022; Accepted 8 July 2022

Available online 11 July 2022

2590-1575/© 2022 The Authors. Published by Elsevier Ltd. This is an open access article under the CC BY-NC-ND license (<http://creativecommons.org/licenses/by-nc-nd/4.0/>).

the specific phytochemicals together, as well in simultaneous dissolve lipophilic molecules from *Z. bungeanum* pericarp, especially the high yield of volatile oil and alkylamides (Arumugham et al., 2021). However, in addition to the extract process involved, simply, the gastric protective effect of SZB has not been reported in depth, especially for the influence of serum metabolism.

In this study, a response surface methodology (RSM) approach, based on the Box-Behnken Design (BBD), was employed to study the optimal conditions for the yield of SC-CO₂ extract from *Z. bungeanum* (SZB). After chemical composition analysis, the protective effect of SZB against gastric disorders induced by cold invading and its serum metabolic profile changes were systematically investigated. The graphical abstract was shown in supplement Fig. S1.

Materials and methods

Materials and reagents

Normal alkane (*n*-alkane, C₁₀-C₂₅) reference substance was purchased from Chengdu Aifa (Chengdu, China). Standards of hydroxy- α -sanshool (>98 %), hydroxy- β -sanshool (>99 %), hydroxy- γ -sanshool (>98 %), hydroxy- ϵ -sanshool (>98 %), hydroxy- γ -isosanshool (>98 %), γ -sanshool (>98 %), dehydro- γ -sanshool (>98 %) were obtained from Chengdu Medesheng (Chengdu, China). *Fuzi Lizhong* pills were purchased from Beijing Tongren Tang (Beijing, China). Enzyme-linked immunosorbent assay (ELISA) kits of Substance P (SP) and Calcitonin gene related peptide (CGRP) were purchased from Nanjing Jiancheng Bioengineering Research (Nanjing, China). Acetonitrile with HPLC grade were purchased from Merck (Darmstadt, Germany).

Experimental design for optimization of SZB

SZB yield (*Y*) defined as amount of oil extract (g) obtained from 100 g dry weight matrix of *Z. bungeanum*, was chosen as the response value for RSM. A BBD with three independent factors including the extract pressure (*A*), temperature (*B*), and time (*C*), each on three levels were performed (Hou, Mu, Ma, & Blecker, 2019) according to the following scheme:

Independent variable	Variable level		
	Low (-1)	Middle (0)	High (+1)
A-Pressure (MPa)	20	25	30
B-Temperature (°C)	35	40	45
C-Time (min)	45	60	75

A total of 17 experiments combinations of the independent variables were shown in supplement Table S1. Design expert software (version 8.0.6) was used to analyze all the experimental data, and the model analysis were performed at a confidence interval of 95 % ($p < 0.05$). When the results showed a saddle point in response surfaces, the estimated ridge of the optimum response was obtained.

GC-MS analysis

Analysis of volatile components of SZB was performed by using an Agilent Technologies chromatograph, series 7890A, with a mass spectrometer (5975C, Agilent Technologies, USA). An HP-5 MS capillary column with 30 m \times 250 μ m \times 0.25 μ m film thickness was used. The temperatures of the ion source was maintained at 230 °C. GC temperature was programmed isothermal at 50 °C for 2 min, then rising from 50 °C to 150 °C at 5 °C/min and maintained for 3 min, and increased to 240 °C at 25 °C/min. The mass spectrometer was operated in the electron-impact mode with ionization energy of 70 eV in a mass range of m/z 50–600. SZB samples were dissolved in *n*-hexane for concentration of 2.021 mg/mL, and samples of 1 μ L were injected with the split ratio of 3:1, at a flow rate of 1.0 mL/min.

The volatile components were identified by comparing their relative retention index (RI) which were obtained by using homologous series of *n*-alkanes (C₁₀-C₂₅) standard and mass spectra (MS) with those recorded in NIST Standard Reference Database (<https://webbook.nist.gov/chemistry/>). The relative percentage of individual compound was determined by normalization method from the GC peak areas, with an assumption of identical mass response factor for all components (Sun et al., 2020a,2020b).

UPLC-Q-Extractive Orbitrap/MS analysis

Analysis of non-volatile components of SZB were performed by using the Vanquish™ UPLC system equipped with Q Exactive™ quadrupole electrostatic field orbitrap high-resolution mass spectrometer (Thermo Fisher Scientific, Massachusetts, USA). Chromatographic separation was achieved using a Thermo Scientific Accucore C₁₈ column (2.1 mm \times 100 mm, i.d. 2.6 μ m) and the injection volume of SZB methanol solution was 3 μ L. Deionized water and acetonitrile, both containing 0.1 % formic acid were used as mobile phases A and B, respectively. The gradient elution program was as follows: 0–15 min, 12 %–38 % B; 15–20 min, 38 %–45 % B; 20–35 min, 45 %–66 % B; 35–50 min, 66 %–98 % B; 50–60 min, 98 % B. The flow rate was 0.3 mL/min, and the column temperature was 30 °C. The mass spectrometer analysis was performed in positive ion mode, with the spray voltage of 3.5 kV. Both the auxiliary gas and the sheath gas were nitrogen, with flow rates of 10 arb and 35 arb, respectively. The capillary temperature and probe heater temperature were set as 320 °C and 350 °C, respectively. Data acquisition was performed in full scan mode of m/z 100–1000. Identification of compounds is usually based on reference standards, chromatographic elution behavior, mass spectrometry fragment patterns.

Animals

Animal experiments were performed in accordance with the guidelines of Ethical Committee for Animal Care and Use of Laboratory Animals of CDUTCM. Male Wistar rats (6-7 weeks old, 200 \pm 20 g) were purchased from SIPEIFU Biotechnology (Beijing, China). All animals were housed 5–6 per cage and kept under standard conditions (25 \pm 2 °C; 55 \pm 5 % humidity) with an alternating 12 h light/dark cycle.

Gastric protective effect of SZB

Gastric disorders model establishment

Gastric disorders model was established as previously described method with some minor modification (Yang, Wen, Zhang, & Liu, 2015). Rats were orally given ice-water mixture (0 °C, 20 mL/kg) twice a day (9:00 a.m. and 9:00 p.m.), which was prepared with ice and water of 2:1, and then maintained at room temperature for 20 min. In addition, a 15 min cold-water bath (10 \pm 1 °C, 10 cm) (1:00 p.m.) were conducted once a day for 14 consecutive days. Normal rats were given the room temperature bathing and an equal volume of normal temperature water in parallel.

Drug administration

Sixty rats were randomly divided into 6 groups ($n = 10$): normal group (0.1 % poloxamer 188 in 0.5 % CMC-Na, p.o.), model group (0.1 % poloxamer 188 in 0.5 % CMC-Na, p.o.), positive group (1000 mg/kg *Fuzi Lizhong* pills, p.o.) and three SZB treatment groups (5, 10 and 20 mg/kg SZB, p.o.). All the drugs were ground with poloxamer 188 and then suspended in 0.5 % CMC-Na. Each rat was orally administrated with corresponding drugs once daily (4:00 p.m.) for 14 consecutive days. The body weight of each rat was measured. The experimental protocol was presented in Fig. 3A.

Sample collection and preparation

All the rats were fasted for 12 h after the last dose, which were then

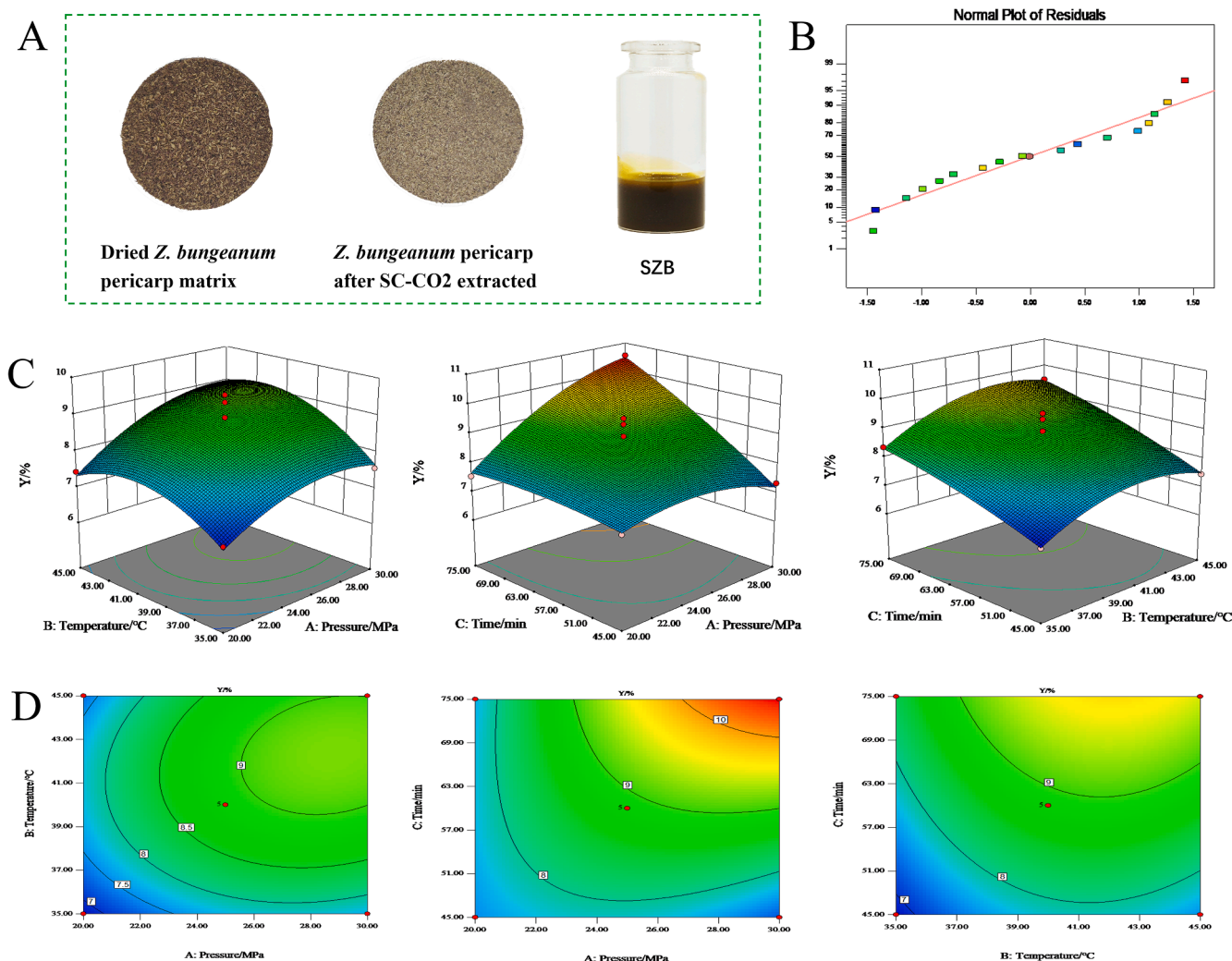


Fig. 1. Optimization of the operative parameters for SZB extract. (A) Macroscopic appearance of the *Z. bungeanum* pericarp matrix before and after SC-CO₂ extract and SZB; (B) Predicted vs observed values for extract yield of SZB; (C) 3-D response surface plots for extract yield of SZB; (D) 2-D contour plots for extract yield of SZB.

anesthetized and sacrificed by intraperitoneal injection of 3 % pentobarbital sodium (2 mL/kg, i.p.). The blood samples were collected through the rat abdominal aorta and static at 4 °C for 2 h. After centrifugation at 3000 rpm for 10 min, the supernatant serum was subpacked and stored at −80 °C for biochemical and metabolomics analysis.

Rat gastric tissue was washed with normal saline and preserved in 4 % paraformaldehyde for pathological examination. The thymus and spleen were removed and weighted, and the viscera indices of which was measured as the weight of the viscera to the body weight (mg/g) of rat.

Extraction of serum metabolite was primarily performed according to previously reported method (Sarafian et al., 2014). Shortly, 100 μL aliquot of each serum sample was mixed with 300 μL precooled methanol and acetonitrile (2:1, v/v), and 10 μL internal standards were added for quality control. After vortexed for 1 min and placed at −20 °C for 2 h, samples were centrifuged at 4000 rpm for 20 min. The 300 μL of supernatant were transferred for vacuum freeze drying, and the dried residue was resuspended with 150 μL methanol and centrifuged for 30 min at 4000 rpm. The aliquot of 5 μL supernatant was injected for metabolomics analysis.

Pathological observation of gastric tissue damage

For pathological observation, the gastric tissue of each group (n = 5) was preserved, dehydrated, and then embedded in paraffin wax. Each tissue block was sectioned at 5-μm thickness using a microtome, and hematoxylin and eosin (HE) staining were performed. After sealing, the

sections were photographed using an optical microscope at 200 to 400 magnifications, which were then evaluated by an experienced pathologist who was blinded to the treatment protocols.

Biochemical index detection

The SP and CGRP level of rat gastric tissue were determined by ELISA kits according to the manufacturer's instructions.

Metabolomics analysis

Serum metabolic profiling data were acquired by a UPLC (Waters, USA) coupled to a Q-Exactive mass spectrometer (Thermo Fisher Scientific, USA) and a heated electrospray ionization (HESI) source. Chromatographic separation was achieved using a Waters ACQUITY UPLC BEH C₁₈ column (2.1 mm × 100 mm, i.d. 1.7 μm) maintained at 45 °C of column temperature. The flow rate was set as 0.35 mL/min and the injection volume was 5 μL. The mobile phase consisted of 0.1 % formic acid in water (A) and 0.1 % formic acid in methanol (B) in the positive ion mode. In the negative mode, 10 mM ammonium formate in water (A) and 10 mM ammonium formate in 95 % methanol (B) were used as the mobile phase. The gradient elution program was as follows: 0–1 min, 2 % B; 1–9 min, 2–98 % B; 9–12 min, 98 % B; 12–12.1 min, 98–2 % B; 12.1–15 min, 2 % B. The ionization source was operated in the positive and negative modes with the flow rates of sheath gas (N₂) and aux gas (N₂) at 40 arb and 10 arb, respectively. The spray voltage was set at 3.8 kV (in positive ion mode) and 3.2 kV (in negative ion mode). The

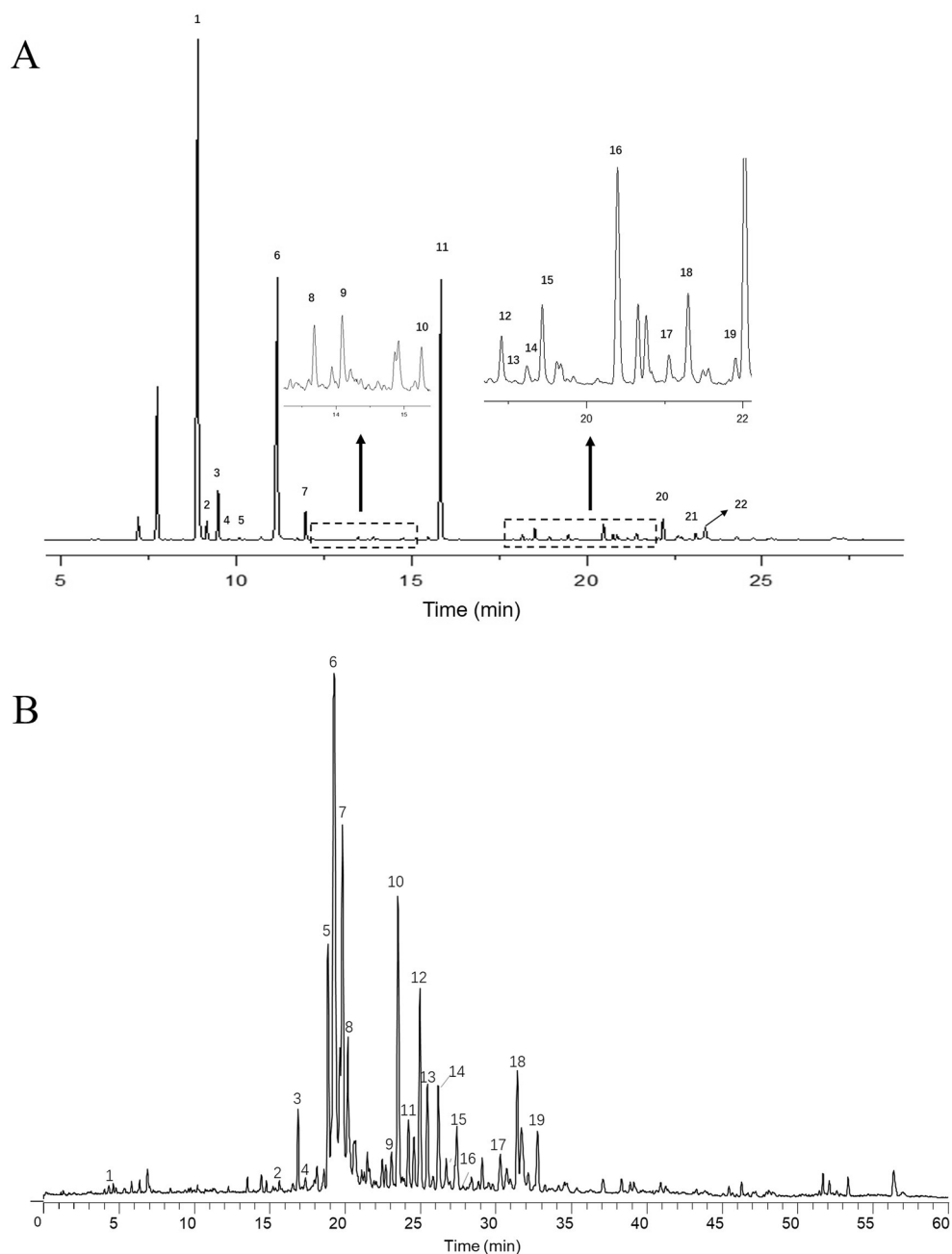


Fig. 2. Total ion chromatogram of SZB by GC-MS (A) and UPLC-Q-Extractive Orbitrap/MS in positive ion mode (B).

full scan range was from 70 to 1050 m/z with a resolution of 70,000 (MS) and 17,500 (MS^2).

A quality control (QC) sample was prepared by mixing equal volume of each serum sample for monitoring the reliability and reproducibility of the analytes found in the samples. QC sample was analyzed consecutively prior to the analytical run and was injected at regular intervals of every 8 samples.

Raw data was firstly analyzed using the Compound Discoverer 3.1 software (Thermo Fisher Scientific, USA). The retention time (RT), m/z values and peak area intensity of each analyst were extracted and were then transferred into R software metaX (Wen, Mei, Zeng, & Liu, 2017) to perform the principal component analysis (PCA) and partial least squares-discriminate analysis (PLS-DA). Differential analysts for group discrimination were obtained from the variable importance in the projection (VIP) and independent t test analysis. Those analysts with $VIP > 1$ and $p < 0.05$ were considered as the significant metabolites and were

identified by comparing with MS/MS analysis, databases of BGI Library, HMDB (<https://www.hmdb.ca/>), and KEGG (<https://www.kegg.jp/>). Pathway analysis was performed with online platform of MetaboAnalyst 5.0, a web-based tool for metabolomics enrichment.

Statistical analysis

Data are presented as mean \pm SD. Statistical differences among all the groups were evaluated by ANOVA followed by LSD test using SPSS 24.0 software (IBM SPSS, USA). The difference was considered as statistically significant at $p < 0.05$.

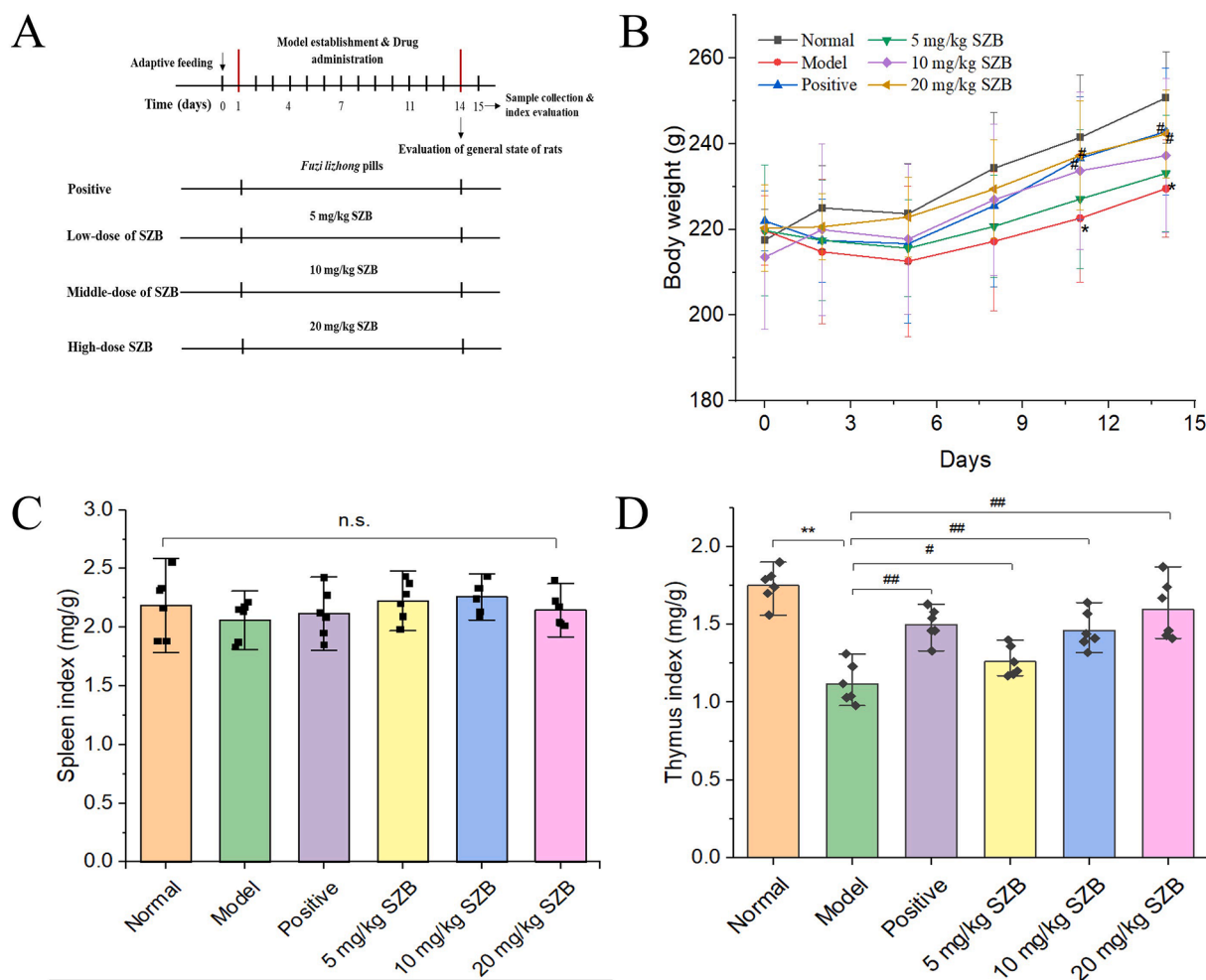


Fig. 3. Protective effect of SZB against gastric disorders in rat body weight and organ index. (A) Experimental protocol of this study; (B) Curve chart variations of rat body weight across time among the six groups; (C) Histogram analysis of spleen index; (D) Histogram analysis of thymus index. Data are expressed as mean \pm SD. * $p < 0.05$ & ** $p < 0.01$ vs normal; # $p < 0.05$ & ## $p < 0.01$ vs model.

Results and discussion

Optimization of SZB extract

The operative parameters including extract pressure, temperature, time and matrix particle size potentially affect the oil yield and recovery of oils rich in bioactive molecules from plant in a reliable SC-CO₂ extraction method (Ishak, Hussain, Coorey, & Ghani, 2021). In this study, results obtained from BBD experiments for yield of SZB (Fig. 1), whose values varied from 6.78 % to 10.54 % (Supplement Table S1), depended on different extract pressure, temperature, and time and their interaction.

ANOVA analysis (Supplement Table S2) showed that the quadratic model is highly significant with a low p value of 0.0057 and F value of 8.15. A non-significant lack of fit ($p = 0.9713$) and an acceptable signal-to-noise ratio (adequate precision = 10.030) were obtained, indicating that the quadratic model can be employed with a low probability of errors. The adjusted R^2 of 0.8008 was in agreement with the predicted R^2 values of 0.7983, which indicates the model explains 80.08 % of response variability. Furthermore, the experiment data was reliable as indicated by a low coefficient of variation (C.V.% = 5.81) and the good agreement of the observed and predicted yield (Fig. 2B). The second-order polynomial equation to express the SZB yield as a function of the coded independent variables was shown below:

$$Y (\text{Yield}) = 8.85 + 0.63A + 0.46B + 0.87C + 0.20AB + 0.77 AC + 0.11BC - 0.48A^2 - 0.67B^2 - 0.16C^2.$$

The equation indicated that extract time had the greatest influence on SZB yield, followed by the pressure ($p < 0.01$) and its interaction with time ($p < 0.05$). These findings were largely expected that increasing pressure could enhance CO₂ density and improve its solubility in the sample, while increasing time within the range has a positive effect in chance of sample.

The SZB yield can also be predicted by 3-D response surface plots and 2-D contour plots, as shown in Fig. 1 C & D, the results of which revealed the nature of the fitted surface as a maximum, a minimum, or a “saddle point”. The SZB extract prepared at 30 MPa/43 °C/75 min was selected for further experiments based on the preferable yield of 10.7 %, taking into consideration a potential final application in food and nutraceutical industries. According to this process, the three times yield of SZB were 10.80 %, 11.30 % and 11.10 %, respectively, with an average value of 11.07 % (RSD = 2.27 %, $n = 3$). This was close to the predicated value of 10.7 % and showed the good reproducibility of the optimized process parameters.

Chemical composition analysis of SZB

Identification of volatile compounds of SZB

As shown in supplement Table S3, in total 22 volatile compounds were determined with retention time from 9.3 min to 23.2 min, and the ionic chromatogram was exhibited in Fig. 2A. These identified compounds accounted for 82.71 % of the total peak area and mainly belonged to the monoterpenoids hydrocarbons (40.26 %), oxygenated

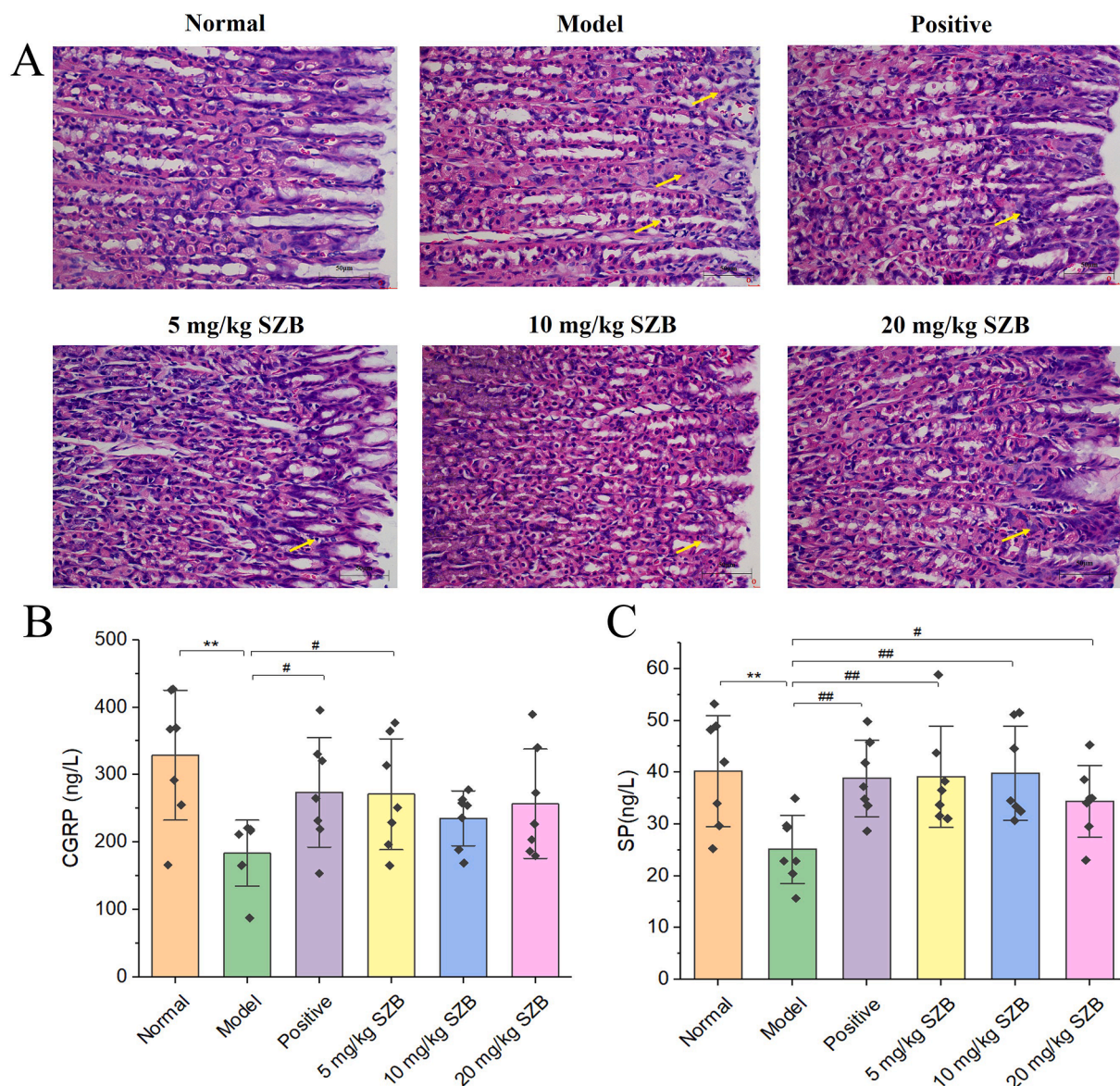


Fig. 4. Protective effect of SZB against gastric disorders on rat pathological changes and biochemical index. (A) H & E staining of gastric tissue (400 ×); (B) Histogram analysis of CGRP content in rat gastric tissue; (C) Histogram analysis of SP content in rat gastric tissue. Data are expressed as mean ± SD. * $p < 0.05$ & ** $p < 0.01$ vs normal; # $p < 0.05$ & ## $p < 0.01$ vs model.

monoterpenes (21.0 %), and ester compounds (16.95 %). The predominant compounds were detected as limonene (34.76 %), linalool (20.45 %) and linalyl acetate (15.65 %), which have been commonly discovered in *Zanthoxylum* species with their representative aroma flavors and documented bioactivity (Sun et al., 2020a,2020b; Yang, 2008). In addition, some smaller amounts such as β -ocimene (2.62 %), germacrene D (1.49 %), and (4E,6Z)-2,6-dimethyl-2,4,6-octatriene (1.46 %) were also found to be the important component of SZB.

Identification of non-volatile compounds of SZB

As shown in Fig. 2B, SZB obtained excellent separation effect and ionization efficiency, and produce $[M + H]^+$ ions in positive mode. Nineteen unsaturated alkylamides including hydroxy-sanshools, dihydroxy-sanshools and bungeanool, were tentatively identified by comparing with the characteristic diagnostic fragment ions of standards and reported literature (Bader, Stark, Dawid, Losch, & Hofmann, 2014; Ji et al., 2019; Ke et al., 2021; Sun et al., 2020a,2020b; Zhang et al., 2019; Zhao et al., 2013). The non-volatile compounds of SZB including the name, formula, RT and main secondary fragment ions were

summarized in supplement Table S4.

The relative abundance of these identified compounds was relatively higher, and No. 6, No. 7 with the largest peak area, were eluted at 19.29 and 19.86 min; the positive ionization mode revealed the same first-order ion $[M + H]^+$ at m/z 264.1958, and similar secondary fragment ions of m/z 246.1850, 147.1168, 107.0858 and 79.0548, which were identified as hydroxy- α -sanshool and hydroxy- β -sanshool (Li et al., 2020), respectively. Although the sanshool derivatives were almost identified in positive mode, it is worthy of attention that there remain other components of SZB in negative ion mode.

Gastric-protective effect of SZB in vivo

Effect of SZB on rat body weight and immune organ indexes

In the present study, an experimental model of gastric disorders induced by oral administration of ice-water mixture and cold-water bath was established. This was reported to be similar to human symptom of gastrointestinal disorders, and can increase the intragastric pressure and elevated the visceral sensitivity in functional dyspepsia-epigastric pain

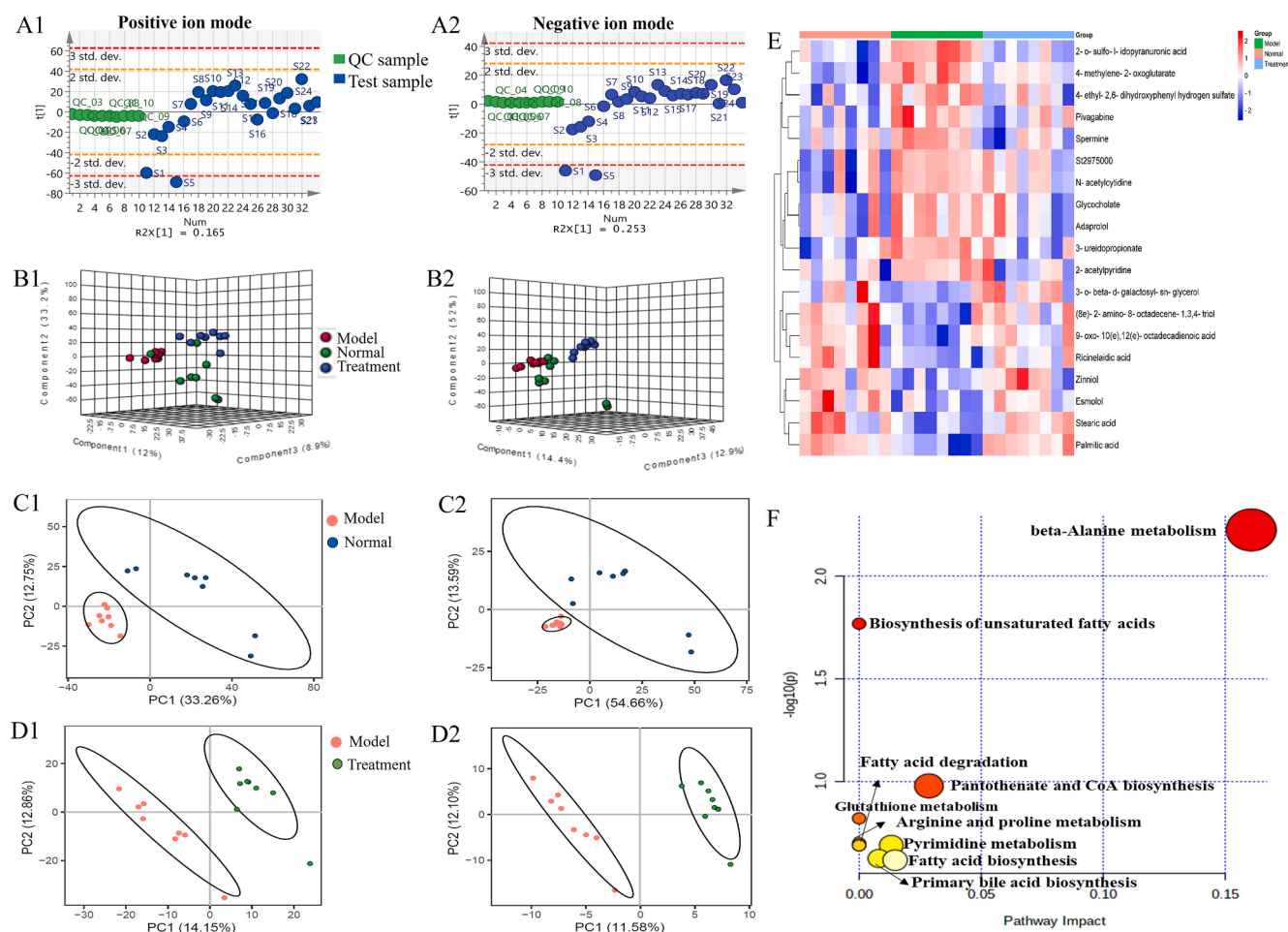


Fig. 5. Differential metabolites and metabolic pathway analysis results. (A) Scores scatter plot of QC and test samples; (B) 3-D PCA score plots; (C) PLS-DA score plots of samples from normal and model group; (D) PLS-DA score plots of samples from model and SZB treatment group; (E) Heatmap visualization for the 19 potential biomarkers; (F) Bubble chart of metabolic pathway analysis.

syndrome (Mustafa & Thulesius, 2001; Wang et al., 2013; Yang et al., 2015). While rats treated with SZB obviously reversed this disorder, at the macro level, as indicated by the increased body weights and organ indexes.

As displayed in Fig. 3B, compared to the normal group, the body weights of rats in the model group were gradually decreased with the prolong of modeling time, especially after 11 days intervention. Whereas, after treatment with 20 mg/kg of SZB, rats body weight was significantly higher than that in the model group ($p < 0.05$) after continuous oral treatment for 11 days, which was similar to the positive group.

Thymus and spleen are the important immune organs which can directly reflect the organism immunity (Wang et al., 2020a, 2020b). In this study, the thymus indexes of model group showed a noticeable decrease ($p < 0.01$) compared with the normal group (Fig. 3D). Interestingly, SZB treatment exhibited similar improvement to positive drug of *Fuzi Lizhong* pills and significant increases of SZB in thymus indexes were observed in a dose-dependent manner, especially at the high dose of 20 mg/kg ($p < 0.01$). There was no obvious difference in spleen index between the normal and model group, as well as the model and SZB treatment group (Fig. 3C).

Effect of SZB on histopathology of gastric tissue

Gastric tissues from normal rats revealed well-preserved intact gastric mucosa, regularly arranged gastric glands and normal round nuclei (Fig. 4A). Compared to the normal group, obvious cell degeneration, cell swelling at the superficial mucosal layer, as well as a few

lymphocytes or eosinophils and small focal necrosis of the gastric mucosa in model group were observed (the yellow arrow points to). However, the rats treated with 10 and 20 mg/kg of SZB and especially those treated with positive drug exhibited slight gastric mucosal lesion with mild edema and cell hyperplasia. These results demonstrated that SZB administration could ameliorated cold-stimulation induced rats gastric tissue damage.

Biochemical analysis

It has been shown that SP and CGRP are involved in sensory signal modulation and play an important role in protecting the stomach against the harmful effect of acrylamide (Palus, Bulc, & Calka, 2018). As shown in Fig. 4B & C, cold stimulation evoked an obvious gastric mucosal lesion as indicated by decreased SP and CGRP levels in rat gastric tissue (by 37.5% and 44.2% compared to the normal control group ($p < 0.01$)). However, the SP level was fully reversed after SZB treatments at doses of 5, 10 and 20 mg/kg and were almost restored to normal levels ($p < 0.05$ & $p < 0.01$), while SZB at 5 mg/kg showed an improved tendency on CGRP level ($p < 0.05$). Meanwhile, positive drug displayed a remarkable improvement in model-induced reduction of SP and CGRP level ($p < 0.01$ & $p < 0.05$).

Metabolomics analysis

Metabolites such as lipids, amino acids, short peptides and nucleic acids are routinely produced by endogenous catabolism (Wishart, 2019). These molecules called “primary” metabolites, play an important role in human health and many key physiological functions (Wang et al.,

Table 1
Nineteen potential biomarkers identified in rat serum which can be regulated by SZB.

No.	Identify	Formula	Adducts	m/z	RT	Mass Error (ppm)	Normal vs Model			Model vs Treatment		
							VIP	P	Trend	VIP	P	Trend
1	Spermine	C ₁₀ H ₂₆ N ₄	[M + H] ⁺	203.2153	0.602	0.42	1.27	0.031	↑*	1.86	0.03	↓ [#]
2	L-iduronate 2-sulfate	C ₆ H ₁₀ O ₁₀ S	[M-H] ⁻¹	272.9917	0.682	1.36	1.38	0.001	↑**	2.70	0.03	↓ [#]
3	2-Methylene-4-oxopentanedioic acid	C ₆ H ₆ O ₅	[M-H] ⁻¹	157.0142	0.693	0.12	1.54	0.002	↑**	1.91	0.008	↓ [#]
4	3- <i>o</i> -beta-D-galactosyl- <i>sn</i> -glycerol	C ₉ H ₁₈ O ₈	[M-H] ⁻¹	268.1152	0.799	0.65	1.39	0.022	↓*	1.09	0.042	↑ [#]
5	3-Ureidopropionate	C ₄ H ₈ N ₂ O ₃	[M + H] ⁺	133.0541	0.944	0.37	1.33	0.024	↑*	2.12	0.008	↓ [#]
6	1,2-Diamino-4-nitrobenzene	C ₆ H ₇ N ₃ O ₂	[M + H] ⁺	154.0614	3.034	-1.69	1.88	0.019	↑*	1.77	0.04	↓ [#]
7	N4-Acetylcytidine	C ₁₁ H ₁₅ N ₃ O ₆	[M + H] ⁺	286.1034	3.034	0.14	1.96	0.019	↑*	1.71	0.04	↓ [#]
8	2-Acetylpyridine	C ₇ H ₇ NO	[M + H] ⁺	122.0602	3.899	-2.21	1.37	0.03	↑*	1.80	0.047	↓ [#]
9	(4-ethyl-2,6-dihydroxyphenyl) Oxidanesulfonic acid	C ₈ H ₁₀ O ₆ S	[M-H] ⁻¹	233.0122	4.339	1.21	1.10	0.005	↑**	1.82	0.02	↓ [#]
10	Pivagabine	C ₉ H ₁₇ NO ₃	[M + H] ⁺	188.1284	5.72	-1.70	1.70	0.007	↑**	2.23	0.045	↓ [#]
11	Zinniol	C ₁₅ H ₂₂ O ₄	[M + H] ⁺	267.1591	6.669	-0.07	1.15	0.004	↓**	1.94	0.043	↑ [#]
12	Esmolol	C ₁₆ H ₂₅ NO ₄	[M + H] ⁺	296.2856	7.242	0.07	1.70	0.004	↓**	1.78	0.03	↑ [#]
13	Glycocholic acid	C ₂₆ H ₄₃ NO ₆	[M + H] ⁺	466.3169	8.176	-0.81	1.60	0.02	↑*	2.68	0.042	↓ [#]
14	Adaprolol	C ₂₆ H ₃₉ NO ₄	[M + H] ⁺	430.2953	8.177	-0.325	1.59	0.027	↑*	2.67	0.047	↓ [#]
15	9-oxo-ODE	C ₁₈ H ₃₀ O ₃	[M + H] ⁺	295.2266	9.014	0.51	1.23	0.02	↓*	1.68	0.041	↑ [#]
16	Dehydrophytosphingosine	C ₁₈ H ₃₇ NO ₃	[M + H] ⁺	316.2845	9.211	0.32	1.30	0.009	↓**	1.62	0.039	↑ [#]
17	Ricinelaidic acid	C ₁₈ H ₃₄ O ₃	[M-H] ⁻¹	297.2432	9.485	0.91	1.35	0.004	↓**	1.61	0.02	↑ [#]
18	Palmitic acid	C ₁₆ H ₃₂ O ₂	[M-H] ⁻¹	256.2402	10.544	-0.42	1.54	0.023	↓*	1.34	0.012	↑ [#]
19	Stearic acid	C ₁₈ H ₃₆ O ₂	[M-H] ⁻¹	283.2714	11.214	0.51	1.28	0.035	↓*	1.12	0.023	↑ [#]

* $p < 0.05$ & ** $p < 0.01$ vs Normal; # $p < 0.05$ & ## $p < 0.01$ vs Model.

2019). In this study, the untargeted metabolic profiling was acquired by representative total ion chromatograms (TICs) of each serum sample (supplement Fig. S2). A total of 2643 compounds in HESI (+) and 780 compounds in HESI (-) were obtained after data pre-processing, and were then subjected to R software for PCA and PLS-DA analysis.

As shown in Fig. 5A, scores scatter plot of QC and test samples in positive and negative mode were mostly within the scope of 3 std except for S1 and S5 sample, which meant a good reproducibility of the detecting system and the high quality of sample data. A clear separation trend among three groups in the 3-D PLS-DA was obtained (Fig. 5B). Obviously, the rat gastric disorder model was successfully replicated from the metabolic perspective, as indicated by the good separation effect between normal and model group in both positive and negative ion modes. Whereas the metabolic profiling in rats treated with SZB was much closer to the normal group, suggesting that SZB played a positive effect in rats with gastric disorder model.

Subsequently, the supervised PLS-DA displayed that the serum samples from the same group clustered together and score plots clearly separated the samples into two blocks between normal and model group, as well as model and treatment group, in both positive and negative ion modes (Fig. 5C & D). The explanation and prediction of PLS-DA model were obtained, of which R²Y and Q² were higher than 0.93 and 0.44 in positive ion mode, and higher than 0.86 and 0.63 in negative ion mode, respectively. These results indicated that the PLS-DA model with satisfactory explanatory and predictive capability is capable of discriminating the different intervention groups.

Based on the parameters of VIP > 1 and $p < 0.05$, a total of 464 differential metabolites were expressed between normal and model group, while 182 were observed between model and SZB treatment group. After intersection and determination, 19 serum metabolites were identified as the potential biomarkers of SZB for protecting rats against cold-stimulated gastric disorder. Compared with the normal group, 11

metabolites were markedly increased in the model group and 8 metabolites were decreased, while these metabolites were reversely regulated after oral administration of SZB. The detailed information of the potential biomarkers was exhibited in Table 1. To visualize the patterns, a heatmap of the potential metabolites in three groups was constructed by using Bioinformatics (<https://www.bioinformatics.com.cn/>), as shown in Fig. 5E. The higher abundant metabolites were shown in red color, while lower abundant metabolites in blue.

Furthermore, the metabolic pathway analyses were performed with MetaboAnalyst 5.0 according to the 19 potential metabolites. As shown in Fig. 5F, 9 metabolic pathways seem contribute to the protective effect of SZB against gastric disorder, including beta-alanine metabolism, glutathione metabolism, pantothenate and CoA biosynthesis, pyrimidine metabolism, biosynthesis of unsaturated fatty acids, primary bile acid biosynthesis.

Nineteen potential metabolites and nine pathways were primarily related to amino acid metabolism and lipid metabolism. Amino acids are essential for various cellular functions and energy source, and participate in metabolic pathways, such as the tricarboxylic acid cycle (TCA) (Kamei, Hatazawa, Uchitomi, Yoshimura, & Miura, 2020). Spermine is one of the polyamine metabolites and is synthesized from ornithine, and the acetylation of spermine could be driven by spermidine. Furthermore, β -alanine could be produced by spermidine through a series of reactions, which was then converted into pyruvate and enters the TCA cycle to regulate tissue energy metabolism (Shimizu et al., 2021). In this study, spermine concentration of serum in model group was significantly increased, whereas it was decreased after SZB treatment for 14 days. It is speculated that spermine was decomposed and involved in the production of β -alanine, subsequently up-regulated β -alanine metabolic pathways, and then promoted energy release.

Lipid metabolism pathway mainly includes unsaturated fatty acid biosynthesis, fatty acid elongation, fatty acid degradation, and primary

bile acid synthesis (Lv et al., 2021). Fatty acids are one of the sources of mammalian, and can be decomposed into H₂O and CO₂ in the body and release a lot of energy. Palmitic acid and stearic acid, the typical saturated fatty acids, involved in body energy metabolism and food digestive absorption (Gangl & Ockner, 1975; Ito et al., 2010). It is reported that acetyl co-enzyme A produced by palmitic acid, could generate CO₂ and ATP (Ramprasad et al., 2001). After SZB intervention, the relative abundance of palmitic acid and stearic acid in serum were elevated, subsequently, which maybe up-regulate the biosynthesis pathway of fatty acids and unsaturated fatty acids, and then decomposes to CO₂ and H₂O under aerobic conditions to releases a lot of energy. Consistent with the research results, Wang et al. (2015) reported that phosphoenolpyruvate hydroxyl kinase could be increased by *Z. bungeanum* treatment, and promote TCA cycle and thereby increasing the internal energy generation (Wang et al., 2015). These findings proved that the protective effect of SZB against gastric disorder not only related to a single metabolic pathway but also a complex network of metabolic pathways. In the network, accelerate energy metabolism of the body is the core mechanism. The main metabolic network of gastric protective effect of SZB was shown in supplement Fig. S3.

Conclusion

Supercritical carbon-dioxide (SC-CO₂) extraction, without use of organic solvents, has been proven to be an effective technology to extract active ingredients of natural plants (Durante et al., 2020). In this study, the effect of extraction influences factors on the oil yield of *Z. bungeanum* were investigated by using response surface methodology (RSM). About 11.07 % yield of SC-CO₂ extract from *Z. bungeanum* (SZB) can be obtained under the optimized parameters of extract pressure (30 MPa), temperature (43 °C) and time (75 min). The major flavor compounds in SZB were determined as limonene, linalool, hydroxy- α -sanshool and hydroxy- β -sanshool by using GC-MS and UPLC-Q-Extractive Orbitrap/MS analysis.

Furthermore, SZB supplementation improved the general growth state of rats with cold-stimulated gastric disorder, as indicated by the increased body weight and visceral index of thymus. It also effectively protected gastric tissue from pathological changes (cell degeneration and swelling). In addition, the metabolic profile of rat serum samples in SZB treatment group was relatively restored by using PCA and PLS-DA analysis. Nineteen differential metabolites such as spermine, glycolic acid, ricinelaic acid, and palmitic acid were identified as the potential biomarkers that contributes to the gastric protective effect of SZB. Taken together, these findings provide a reliable basis for supporting the health function of SZB, obtained by a green extract technique-supercritical CO₂ extract, for good application potential in the development of food and health products.

CRediT authorship contribution statement

Mengmeng Zhang: Conceptualization, Writing – original draft. **Daneng Wei:** Conceptualization, Writing – original draft. **Lin He:** Conceptualization, Writing – original draft. **Dan Wang:** Supervision. **Li Wang:** Supervision. **Dandan Tang:** Writing – review & editing. **Rong Zhao:** Investigation, Software. **Xun Ye:** Investigation, Software. **Chunjie Wu:** Writing – review & editing, Funding acquisition. **Wei Peng:** Writing – review & editing.

Declaration of Competing Interest

The authors declare that they have no known competing financial interests or personal relationships that could have appeared to influence the work reported in this paper.

Acknowledgements

The authors acknowledge the financial support provided by Sichuan Provincial Administration of Traditional Chinese Medicine (2020HJZX001).

Appendix A. Supplementary data

Supplementary data to this article can be found online at <https://doi.org/10.1016/j.fochx.2022.100391>.

References

- Arumugham, T., Rambabu, K., Hasan, S. W., Show, P. L., Rinklebe, J., & Banat, F. (2021). Supercritical carbon dioxide extraction of plant phytochemicals for biological and environmental applications-a review. *Chemosphere*, 271, Article 129525.
- Bader, M., Stark, T. D., Dawid, C., Losch, S., & Hofmann, T. (2014). All-trans-configuration in Zanthoxylum alkylamides swaps the tingling with a numbing sensation and diminishes salivation. *Journal of Agriculture and Food Chemistry*, 62(12), 2479–2488.
- Durante, M., Ferramosca, A., Treppiccione, L., Di Giacomo, M., Zara, V., Montefusco, A., ... Lenucci, M. S. (2020). Application of response surface methodology (RSM) for the optimization of supercritical CO₂ extraction of oil from pate olive cake: Yield, content of bioactive molecules and biological effects in vivo. *Food Chemistry*, 332, Article 127405.
- Gangl, A., & Ockner, R. K. (1975). Intestinal metabolism of plasma free fatty acids. Intracellular compartmentation and mechanisms of control. *Journal of Clinical Investigation*, 55(4), 803–813.
- Hou, F., Mu, T., Ma, M., & Blecker, C. (2019). Optimization of processing technology using response surface methodology and physicochemical properties of roasted sweet potato. *Food Chemistry*, 278, 136–143.
- Ishak, I., Hussain, N., Coorey, R., & Ghani, M. A. (2021). Optimization and characterization of chia seed (*Salvia hispanica* L.) oil extraction using supercritical carbon dioxide. *The Journal of CO2 Utilization*, 45, Article 101430.
- Ito, M., Jaswal, J. S., Lam, V. H., Oka, T., Zhang, L. Y., Beker, D. L., ... Rebeyka, I. M. (2010). High levels of fatty acids increase contractile function of neonatal rabbit hearts during reperfusion following ischemia. *American Journal of Physiology-Heart and Circulatory Physiology*, 298(5), H1426–H1437.
- Kamei, Y., Hatazawa, Y., Uchitomi, R., Yoshimura, R., & Miura, S. (2020). Regulation of skeletal muscle function by amino acids. *Nutrients*, 12(1), 261.
- Ke, J., Cheng, J., Luo, Q., Wu, H., Shen, G., & Zhang, Z. (2021). Identification of two bitter components in *Zanthoxylum bungeanum* Maxim. and exploration of their bitter taste mechanism through receptor hTAS2R14. *Food Chemistry*, 338, Article 127816.
- Kubota, K., Ohtake, N., Ohbuchi, K., Mase, A., Imamura, S., Sudo, Y., ... Uezono, Y. (2015). Hydroxy- α sanshool induces colonic motor activity in rat proximal colon: A possible involvement of KCNK9. *American Journal of Physiology. Gastrointestinal and Liver Physiology*, 308(7), G579–G590.
- Li, W., Wu, Y., Liu, Y., Tang, Y., Che, Z., & Wu, T. (2020). Chemical profiles and screening of potential α -glucosidase inhibitors from Sichuan pepper using ultra-filtration combined with UHPLC-Q-TOF. *Industrial Crops and Products*, 143, Article 111874.
- Lv, X. C., Chen, M., Huang, Z. R., Guo, W. L., Ai, L. Z., Bai, W. D., ... Ni, L. (2021). Potential mechanisms underlying the ameliorative effect of *Lactobacillus paracasei* FZU103 on the lipid metabolism in hyperlipidemic mice fed a high-fat diet. *Food Research International*, 139, Article 109956.
- Moraes, T. M., Kushima, H., Moleiro, F. C., Santos, R. C., Machado Rocha, L. R., Marques, M. O., ... Hiruma-Lima, C. A. (2009). Effects of limonene and essential oil from Citrus aurantium on gastric mucosa: Role of prostaglandins and gastric mucus secretion. *Chemico-Biological Interactions*, 180(3), 499–505.
- Mustafa, S. M., & Thulesius, O. (2001). Cooling-induced gastrointestinal smooth muscle contractions in the rat. *Fundamental & Clinical Pharmacology*, 15(5), 349–354.
- Ni, R. J., Yan, H. Y., Tian, H. L., Zhan, P., & Zhang, Y. Y. (2022). Characterization of key odorants in fried red and green huajiao (*Zanthoxylum bungeanum* maxim. and *Zanthoxylum schinifolium* sieb. et Zucc.) oils. *Food Chemistry*, 377, Article 131984.
- Palus, K., Bulc, M., & Calka, J. (2018). Changes in VIP-, SP- and CGRP- like immunoreactivity in intramural neurons within the pig stomach following supplementation with low and high doses of acrylamide. *Neurotoxicology*, 69, 47–59.
- Sarafian, M. H., Gaudin, M., Lewis, M. R., Martin, F. P., Holmes, E., Nicholson, J. K., & Dumas, M. E. (2014). Objective set of criteria for optimization of sample preparation procedures for ultra-high throughput untargeted blood plasma lipid profiling by ultra performance liquid chromatography-mass spectrometry. *Analytical Chemistry*, 86(12), 5766–5774.
- Shimizu, H., Usui, Y., Wakita, R., Aita, Y., Tomita, A., Tsubota, K., ... Goto, H. (2021). Differential tissue metabolic signatures in IgG4-related ophthalmic disease and orbital mucosa-associated lymphoid tissue lymphoma. *Investigative Ophthalmology & Visual Science*, 62(1), 15.
- Sun, J., Sun, B., Ren, F., Chen, H., Zhang, N., & Zhang, Y. (2020a). Characterization of key odorants in Hanyuan and Hancheng fried pepper (*Zanthoxylum bungeanum*) oil. *Journal of Agriculture and Food Chemistry*, 68(23), 6403–6411.
- Sun, X., Zhang, D., Zhao, L., Shi, B., Xiao, J., Liu, X., ... Zou, X. (2020b). Antagonistic interaction of phenols and alkaloids in Sichuan pepper (*Zanthoxylum bungeanum*) pericarp. *Industrial Crops and Products*, 152, Article 112551.

- Wang, X., Gao, Y., Tian, Y., Liu, X., Zhang, G., Wang, Q., ... Wang, Q. (2020a). Integrative serum metabolomics and network analysis on mechanisms exploration of Ling-Gui-Zhu-Gan Decoction on doxorubicin-induced heart failure mice. *Journal of Ethnopharmacology*, 250, Article 112397.
- Wang, Z. H., Lin, Y., Jin, S., Wei, T. N., Zheng, Z. H., & Chen, W. M. (2020b). Bone marrow mesenchymal stem cells improve thymus and spleen function of aging rats through affecting P21/PCNA and suppressing oxidative stress. *Aging-Us*, 12(12), 11386–11397.
- Wang, R. F., Wang, Z. F., Ke, M. Y., Fang, X. C., Sun, X. H., Zhu, L. M., & Zhang, J. (2013). Temperature can influence gastric accommodation and sensitivity in functional dyspepsia with epigastric pain syndrome. *Digestive Diseases and Sciences*, 58(9), 2550–2555.
- Wang, Q. H., Yang, X., Li, X. L., Yang, B. Y., Wang, Y. H., & Kuang, H. X. (2015). Based on proteomics to study the property and flavor of Radix Aconiti Lateralis Preparata, Rhizoma Zingiberis, Pricklyash Peel. *World Chinese Medicine*, 10(12), 1824–1836.
- Wen, B., Mei, Z., Zeng, C., & Liu, S. (2017). MetaX: A flexible and comprehensive software for processing metabolomics data. *BMC Bioinformatics*, 18(1), 183.
- Wishart, D. S. (2019). Metabolomics for investigating physiological and pathophysiological processes. *Physiological Reviews*, 99(4), 1819–1875.
- Yang, X. (2008). Aroma constituents and alkylamides of red and green huajiao (*Zanthoxylum bungeanum* and *Zanthoxylum schinifolium*). *Journal of Agriculture and Food Chemistry*, 56(5), 1689–1696.
- Yang, W. B., Wen, B., Zhang, L. H., & Liu, H. (2015). Establishment of animal model with gastric cold syndrome. *Zhongguo Zhong Yao Za Zhi*, 40(20), 4031–4036.
- Zhang, M. M., Wang, J. L., Zhu, L., Li, T., Jiang, W. D., Zhou, J., ... Wu, C. J. (2017). *Zanthoxylum bungeanum* Maxim. (Rutaceae): A systematic review of its traditional uses, botany, phytochemistry, pharmacology, pharmacokinetics, and toxicology. *International Journal of Molecular Sciences*, 18(10), 2172.
- Zhang, L. L., Zhao, L., Wang, H. Y., Shi, B. L., Liu, L. Y., & Chen, Z. X. (2019). The relationship between alkylamide compound content and pungency intensity of *Zanthoxylum bungeanum* based on sensory evaluation and ultra-performance liquid chromatography-mass spectrometry/ mass spectrometry (UPLC-MS/MS) analysis. *Journal of the Science of Food and Agriculture*, 99(4), 1475–1483.
- Zhao, Q., Xu, W., Wang, G., & Zhao, E. (2021). Research progress on extraction process and bioactivity of oleoresin from *Zanthoxylum bungeanum*. *Cereals & Oils*, 34(1), 4–7.
- Zhao, Z. F., Zhu, R. X., Zhong, K., He, Q., Luo, A. M., & Gao, H. (2013). Characterization and comparison of the pungent components in commercial *Zanthoxylum bungeanum* oil and *Zanthoxylum schinifolium* oil. *Journal of Food Science*, 78(10), 1516–1522.